Damage Measures for Performance-Based Design of Rectangular Concrete-Filled Steel Tube Members and Connections

Cenk TORT[1] and Jerome F. HAJJAR[2]

SUMMARY

Damage evolution of rectangular concrete-filled steel tube (RCFT) column and beam-column members as documented in experimental tests is presented in this paper. An experimental database was first constructed that included RCFT tests available in the worldwide literature. Based on the experimental data, appropriate damage states for RCFT members, connections, and frames were defined at different levels of loading. For each damage state, the performance of the specimens was documented quantitatively with the use of damage and ductility functions developed in this work. The paper then documents how to use these damage measures to assess the capacity of RCFT columns and beam-columns within the context of a performance-based design methodology.

***Keywords**: rectangular concrete-filled steel tube, composite column, composite beam-column, composite connection, damage function, damage index, performance-based design, earthquake engineering, seismic.*

INTRODUCTION

Rectangular concrete-filled steel tube (RCFT) beam-columns are increasingly being used in the lateral resistance frames of high-rise buildings (Hajjar, 2000). The excellent cyclic performance and potential economical benefits of RCFTs requires developing improved design provisions for assessing the behavior of RCFT members with adequate reliability, particularly for seismic loading. A wide range of experimental and analytical research has been done on RCFTs over the last decade (Gourley et al., 2001; Morino et al., 2001). In addition, performance-based design (PBD) principles have started to be developed for composite structures (Mehanny and Deierlein, 2000). In this work, the first phase of research towards developing PBD guidelines for composite RCFT structures will be presented. A database study documenting worldwide test results on RCFT members will first be described. Next, using the available results in the database, the damage evolution of the RCFT specimens in the database will be investigated using damage functions. Finally, a design methodology incorporating these damage functions will be presented within the context of PBD principles.

DEVELOPMENT OF EXPERIMENTAL RCFT DATABASE

The well-documented experimental work from around the world on RCFT members was compiled into two databases, including monotonically-loaded experiments and cyclically-loaded experiments. A database was developed for each significant type of RCFT component, including RCFT columns, beam-columns, panel zones, pinned connections, moment-resisting connections, and frames. Monotonically- and cyclically-loaded columns and beam-columns constitute the majority of the specimens in the literature, and will be the focus of this paper.

In each database, information about the key geometric and material properties of the specimens (e.g., yield strength of steel tube (f_y), compressive strength of concrete (f'_c), modulus elasticity of steel (E_s), depth (D), thickness (t), length (L), etc.) was recorded, including both nominal and measured values. The boundary conditions and test-setup of the specimens were also described in the database. In addition, force and displacement values (including detailed information on the quarter-cycle number, etc., where relevant) were

[1] *Graduate Research Assistant, Department of Civil Engineering, University of Minnesota, Minneapolis, USA, email: tort0008@umn.edu*
[2] *Associate Professor, Department of Civil Engineering, University of Minnesota, Minneapolis, USA, email: hajjar@struc.ce.umn.edu*

recorded for the point of peak response and for the occurrence of each significant type of local damage (e.g. steel yielding, steel local buckling, concrete crushing, etc.). Similar local damage levels were defined for the monotonic and cyclic tests to permit direct comparison.

DAMAGE ASSESSMENT OF RCFT MEMBERS

In performance-based design, the design of structures is often carried out according to multiple performance objectives. A performance objective has two components, including a performance level and a hazard level. A performance level characterizes the damaged state of the structure, which typically levels ranging from Immediate Occupancy through Life Safety, Near Collapse, and Collapse Prevention (FEMA, 1997; FEMA, 2000). A hazard level corresponds to the seismic load given as a recurrence interval or a probability of exceedance within a specified number of years (e.g. 50% probability of exceedance within 50 years, or approximately a 75 year recurrence interval).

For each performance objective, acceptance criteria must be developed, which in past work are commonly related to a limiting interstory drift ratio (Yun et al., 2002). In this research study, damage functions were employed to characterize the performance levels. Deformation-based and energy-based measures (e.g., axial deformation, interstory drift, and their corresponding force values, etc.) were selected as the operating variables for the damage functions. For each specimen existing in the database, the damage evolution was examined by quantifying the damage functions at the time of occurrence of the local damage levels (e.g. steel yielding, local buckling, etc.). This task provided quantified data on the occurrence of damage and helped to associate local damage states to the performance levels.

Two types of damage functions were thus developed for monotonically-loaded RCFT members. The first damage function was deformation-based (D), for which the damage was defined as the ratio of deflection at the point in the loading history at which damage is being assessed (d_{curr}) to the deflection attained when the peak load is reached (d_o) (with the specific type of load and deflection being assessed varying with the type of test) as given in Equation 1. This damage function normalizes to a value of 1.0 if the damage state occurs at a deformation level when the peak load is achieved:

$$D = d_{curr} / d_o \tag{1}$$

The second damage function was developed as energy-based (E), for which the damage was defined as the ratio of the energy absorption at the point in the loading history at which the damage is being assessed (E_{curr}) to the total energy absorption at the end of the test (E_{total}), as given in Equation 2:

$$E = E_{curr} / E_{total} \tag{2}$$

The end of the test was determined depending on the load-deflection characteristics of the specimens in the post-peak region. For the RCFT members undergoing large deformation and exhibiting a softening or hardening type of post-peak response, the end of test was taken as the point where the stiffness of the specimens in the post-peak region approaches zero. It is also typical for RCFT members to have an elastic-perfectly plastic response without any significant strength change after the peak. In this case, the end of test was determined based on a limiting deflection value that was taken as 6% drift for the beam-column, connection, and frame tests. If RCFT members exhibit an abrupt failure, the end of test was assumed to be the last point on the experimental load-deflection curve.

In the case of cyclically-loaded RCFT tests, only an energy-based damage function was utilized. The function was adopted from the damage function of Kradzig et al. (1989), which is given in Equation 3:

$$E = E^+ - E^+E^- + E^- \tag{3a}$$

$$E^+ = \frac{\sum E_{si}^+ + \sum E_i^+}{E_u^+ + \sum E_i^+} \tag{3b}$$

$$E^- = \frac{\sum E_{si}^- + \sum E_i^-}{E_u^- + \sum E_i^-} \tag{3c}$$

where

E^+ – intermediate variable for positive direction of loading
E^- – intermediate variable for negative direction of loading
E_i^+ – energy dissipation in positive primary half cycles
E_i^- – energy dissipation in positive primary half cycles
E_{si}^+ – energy dissipation in positive secondary half cycles
E_{si}^- – energy dissipation in negative secondary half cycles
E_u^- – normalizing factor for negative deformation
E_u^+ – normalizing factor for positive deformation

It was assumed in this work that the damage of the RCFT members is mainly caused by primary half cycles and the effect of secondary cycles in damaging the specimens was neglected [see Figure 1 for a definition of primary and secondary cycles by (Kradzig et al., 1989)]. In addition, due to symmetry of the RCFT members, the intermediate variables in the positive and negative directions were treated separately rather than combining them to give a single damage index value. This resulted in Equation 4 as the damage function used to quantify the damage in the cyclic tests:

$$E = E^+ = E^- = \frac{E_{cb}}{E_m} \tag{4}$$

where

E_{cb} - area under the cyclic back-bone curve until the point at which damage is assessed
E_m - area under the complete cyclic back-bone curve

For the specimens in the database, E_{cb} was calculated from the experimental cyclic load-deflection curves after connecting the peak points at each cycle. On the other hand, E_m was calculated from the monotonic load-deflection curve of the specimens, which was determined either analytically [e.g., using finite element analysis based upon the use of a concentrated plasticity model (Hajjar et al., 1997)] or by using empirical formulations for the backbone curves developed from the experimental data (Tort and Hajjar, 2003).

The damage functions given in Equations 1, 2, and 4 were evaluated for the specimens in the database at the occurrence times of the local damage states. This quantified data for damage provided information to compare the sequence and likely time of occurrence of the local damage states. In addition, the reserve strength of the specimens after local damage took place was also examined based on the damage index values and based upon the available ductility of the specimens. The displacement ductility (μ) of the specimens in the database was calculated as the ratio of the displacement at an appropriate limiting value for ductility assessment (Tort and Hajjar, 2003) to the yield displacement. Displacement measures such as axial deflection (δ) and chord rotation (R) were utilized to assess ductility. For every member type categorized in the database, equations were then derived to estimate the member ductility in terms of RCFT structural parameters. As an example Equation 5 was derived to calculate the ductility of monotonic beam-column specimens that were fixed at each end, subjected to constant axial compression, and subjected to shear to put the member in double curvature:

$$\mu = -0.32 \times (L / D) - 3.78 \times (P_c / P_o) - 0.28 \times (P / P_o) + 23.24 \tag{5}$$

where

P –axial compression force
P_c – nominal strength of concrete core
P_o – nominal strength of composite section

Tort and Hajjar (2003) present similar equations, along with their limits of applicability, for RCFT members and connections.

For the sake of brevity, in the present paper, the damage assessment study will only be presented for selected examples from monotonically-loaded columns, monotonically-loaded beam-columns and cyclically-loaded beam-columns. Tort and Hajjar (2003) present a similar damage assessment study for other RCFT components, including panel zones, pinned connections, moment-resisting connections, and frames.

Monotonically-Loaded Columns

The monotonically-loaded column database covered stocky and slender specimens tested under concentrically applied axial load. The damage levels investigated for the RCFT column specimens were identified as steel

yielding, concrete crushing, and local buckling. Steel yielding and concrete crushing points on the load-deflection curves were determined by supplementing the results reported directly from the experiments with analytical procedures to generate the required data. Local buckling points were determined by direct reporting from the experimental results.

For the monotonically-loaded column tests, both deformation-based and energy-based damage functions were evaluated. Equations were derived to estimate the damage index values that were attained at the occurrence time of the local damage states. For example, Equation 5 was developed to estimate the deformation-based damage index value when local buckling takes place, where it can be seen that d_{lb}/d_o reduces as $(D/t)\times\sqrt{f_y/E_s}$ increases.

$$d_{lb}/d_o = 2.68\times((D/t)\times\sqrt{f_y/E_s})^{-1.02} \tag{6}$$

where

d_{lb} – deformation at local buckling

Similar types of equations were derived for both deformation- and energy-based damage functions for all of the local damage states (e.g., yielding (d_{cy}/d_o, E_{cy}/E_{total}), concrete crushing (d_c/d_o, E_c/E_{total}), and local buckling (E_{lb}/E_{total})). For the monotonically-loaded column tests, the summary of all the damage functions, including their limits of applicability for key RCFT parameters (f_y, f'_c, D/t, etc.) and statistical properties [number of data points (N), coefficient of correlation (R^2), mean value (η), and standard deviation (σ)] can be seen in Table 1. Similar types of tables were generated for every member type in the database. In this paper, only the equations table for monotonically-loaded column tests are presented for conciseness.

Monotonically-Loaded Beam-Columns

In the literature, four types of monotonically-loaded beam-column specimens were identified depending on the type of loading as listed below:

MI – eccentrically applied monotonic axial compression (single curvature, proportional loading)
MII – constant axial compression and monotonic shear at the ends (double curvature, proportional loading)
MIII – constant axial compression and uniform flexure (single curvature, nonproportional loading)
MIV – four point bending (single curvature, proportional loading)

For brevity, only MII type beam-columns that were tested under constant axial compression (P) and monotonically increasing shear force (V) will be presented.

For MII type beam-columns, the common damage levels reported in the tests are compression yielding, tension yielding, local buckling in the flange, and local buckling in the web. These damage levels were determined by direct assessment of the damage levels as reported in the experiments. The moment and chord rotation were the key load and deformation measures used to create the damage functions. Concrete cracking and concrete crushing could not be discerned accurately from the experiments in the database.

For example, Equation 7 was derived to estimate the energy-based damage index for yielding of the tension flange using the data obtained from the tests:

$$\frac{E_{ty}}{E_{total}} = 0.62\frac{P}{P_o} - 0.16\frac{P_s}{P_o} + 0.039 \tag{7}$$

where

E_{ty} – energy at yielding of the tension flange
P_s – nominal strength of steel tube

Figure 2 plots the variation of E_{ty}/E_{total} for the data used to derive Equation 7. Ductility values are shown superimposed on each experimental point. A corresponding plot for the associated deformation-based damage index was generated (Tort and Hajjar, 2003), which shows that tension flange yielding occurs in the vicinity of the peak load. It can also be seen from the figure that beam-columns in which the concrete is dominant (i.e., high D/t or, equivalently, low P_s/P_o, thus having thin-walled steel tubes) experience tension flange yielding at a larger damage level as compared to their counterparts with thick-walled steel tubes. This phenomenon can be attributed to the fact that for members having thin walled or low strength steel tubes, where the concrete

contribution to the overall behavior is significant, the steel tube takes a smaller share of the applied loading, and thus yielding is delayed. The data also indicate that as the axial load applied to the beam-column members increases, tension flange yielding is delayed, causing the damage index to increase, as would be expected. The superimposed ductility values also clarify that the beam-columns have significant post-peak ductility. It is by viewing the deformation-based damage function, energy-based damage function, and ductility values together that a complete picture of the trends in this damage state may be quantified for performance-based design. These values indicate that the damage state occurs in the range of the peak load, but that the damage is not catastrophic, as significant post-peak energy and ductility are documented. Further comparison of this type of information with similar data for the other beam-column damage states, as is done below in the parametric study, provides a complete picture of the progression and characteristics of damage in RCFT members and connections.

Cyclically-Loaded Beam-Columns

The cyclically-loaded beam-column specimens recorded in the database were all tested under constant axial load and cyclically applied shear load (similar to the MII loading scheme). The damage levels observed during the tests were similar to their monotonic counterparts. The damage levels during the experiments were determined either through direct assessment from the experimental load-deflection curves, or by supplementing the results reported directly from the experiments with analytical procedures to generate the required data. The damage levels of concrete cracking, compression yielding and tension yielding were detected on the experimental load-deflection curves by running a moment-curvature analysis, while the damage levels of concrete crushing and local buckling were all determined by direct assessment from the experimental load-deflection curves.

Figure 3 shows the results from the damage assessment study for local buckling in the steel tube flange. It can be seen from Figure 4 that the damage index values show a decreasing trend for larger values of $(D/t)\times\sqrt{f_y/E_s}$. However, unlike for monotonically-loaded beam-columns, no clear trend was observed for the effect of axial load on the damage index value, indicating that the flexural response to the cyclic loading dominates the local buckling progression in these RCFT beam-columns (for the applicable range of P/P_o).

PARAMETRIC STUDY

A parametric study was conducted for each member type using the equations of the damage indices. For this purpose, multiple specimens were generated based on the limits of the damage index equations for the RCFT material and geometric properties. For each generated specimen, the damage indices at the local damage levels were then evaluated and plotted on the same graph. An example is given of the results for RCFT columns.

For the monotonically-loaded column tests, a total of 16 RCFT members were used, having varying structural parameters that included D/t, L/D, f'_c and f_y. The geometric and material parameters for all 16 RCFT members used in this study are presented in Table 2. Table 2 also reports the deformation-based damage function values and calculated ductility of the specimens. In Figure 4, the results of the parametric study for the deformation-based damage indices of the monotonically-loaded column tests are shown. It was found that the steel yielding and concrete crushing damage levels generally occur at approximately the same time in the pre-peak region with a deformation-based damage index of approximately 0.5, except for cases where P_c/P_o is high (e.g., specimens 3 through 8 in Table 5), for which concrete crushing is delayed further. Local buckling was found to occur later, particularly for specimens having low D/t and low f_y values (e.g., specimens 1 through 4 and 9 through 12 in Table 5). Local buckling in the pre-peak region is noted if the specimens have large D/t ratios and high f_y values (e.g., specimens 13 through 16 in Table 5). High D/t and high f'_c, resulting in a high P_c/P_o ratio, generally were the most significant cause for reduced ductility (e.g., Specimens 3 through 8, 15, and 16, in Table 5). Note that while overall flexural buckling was recorded for these specimens, a damage index was not established for this limit state as it is commonly covered by other equations (e.g., a column curve) in current specifications (AISC, 2002) that would likely be incorporated into any performance-based specification.

INTENDED PERFORMANCE-BASED DESIGN METHODOLOGY

A reliability-based performance evaluation (e.g., Yun et al., 2002) similar to FEMA (2000) is intended as a next step in this work, using the results presented above for damage assessment of RCFT members and connections. The intended methodology is described in Figure 5. The design of an RCFT member starts by selecting an appropriate performance level (e.g. Immediate Occupancy, Life Safety etc.). Using the equations such as those given in Table 1 (Tort and Hajjar, 2003), the damage indices ($D_{capacity}$, $E_{capacity}$) per RCFT member are calculated

at each local damage level. The local damage levels are then mapped onto performance levels based on a scale given in Table 3. Similar scales were presented by Mehanny and Deierlein (2000) for composite structures. While their energy-based damage scale was derived mainly for reinforced concrete columns and composite girders, the range of values identified in Table 3 was found in this research to work well for RCFT components. The deformation-based scale is similar to that presented by Mehanny and Deierlein (2000), but was adjusted because their deformation-based index was based upon a ductility measurement and thus was defined slightly differently from that used in this work. Through this table, it may be determined which damage states should be checked per member for the selected performance objective. In the second stage given in Figure 5, the load-deflection curve of the designed member is constructed. This is achieved through finite element analysis (Hajjar et al., 1997) or empirical formulations derived in this work (Tort and Hajjar, 2003). In Stage III, the structure is analyzed under earthquake loading with an analysis approach permitted in the design provisions (e.g., equivalent static load). From the analysis results, the peak deflection (e.g., interstory drift (R_{max})) is extracted and the current state of the member is located on the load-deflection curve prepared in Stage II. The deformation-based (D_{demand}) or energy-based (E_{demand}) damage index values are then calculated using the demand parameters. In Stage IV, all the damage indices are adjusted for the demand (γ) and resistance (ϕ) factors, D_{demand} and E_{demand} are then checked versus the limits determined in Stage I ($D_{capacity}$, $E_{capacity}$).

SUMMARY AND CONCLUSIONS

In this paper, an experimental database study of RCFT members was presented. The database covered both monotonic and cyclic tests from the literature. Damage assessment of the specimens from the database was then documented through the development of deformation-based and energy-based damage functions. Functions expressing the member ductility as a function of key structural parameters of RCFT members were similarly derived. Based on observations from the quantified data on damage, the following conclusions were drawn:

1. The deformation-based damage functions provide information on the occurrence of damage relative to achieving the peak strength of the member, while the energy-based damage functions quantify the amount of reserve strength available after damage occurs. When coupled with ductility measures, these functions provide an efficient and comprehensive way of quantifying damage in RCFT members and connections.

2. The local damage levels identified for RCFT members, such as concrete cracking, concrete crushing, steel yielding, and local buckling, exhibit complex relationships. The composite interaction between steel and concrete was quantified in the proposed equations by correlating the damage levels related to the composite characteristics of the RCFTs using non-dimensional parameters (e.g., D/t, P_s/P_o, P_c/P_o).

3. A parametric study of RCFT members was conducted to enable comparison of the occurrence of each damage state relative to each other, and to identify which damage states are appropriate for checking for each performance level. An approach was then presented for classifying each damage state of RCFT members according to performance levels ranging from Immediate Occupancy to Collapse Prevention, with most of the damage states being appropriate for Immediate Occupancy, Life Safety, or Near Collapse.

4. This research provides a first step for establishing reliability-based performance-based design provisions for rectangular concrete-filled steel members and frames. The damage functions generated in this work, simplified as needed for final design implementation and coupled with corresponding assessment of demand in ongoing research, provide the necessary information for creating a comprehensive performance-based design procedure for RCFTs for performance levels ranging from Immediate Occupancy to Collapse Prevention. The performance-based design method proposed in this work, which fits most directly into a displacement-based design approach, thus augments the traditional strength-based design methodologies that are used in current design specifications [e.g., (AISC, 2002)].

REFERENCES

American Institute of Steel Construction (AISC) (2002). *Seismic Provisions for Structural Steel Buildings*, AISC, Chicago, Illinois.

Federal Emergency Management Agency (FEMA) (1997). *NEHRP Guidelines for the Seismic Rehabilitation of Buildings*, FEMA 273, Federal Emergency Management Agency, Washington, D.C.

Federal Emergency Management Agency (FEMA) (2000). *Recommended Seismic Design Criteria for New Steel Moment-Frame Buildings*, FEMA 350, Federal Emergency Management Agency, Washington, D.C.

Gourley, B. C., Tort, C., Hajjar, J. F., and Schiller, P. H. (2001). "A Synopsis of Studies of the Monotonic and Cyclic Behavior of Concrete-Filled Steel Tube Beam-Columns," Structural Engineering Report No. ST-01-4, Department of Civil Engineering, University of Minnesota, Minneapolis, Minnesota, Version 3.0, December.

Hajjar, J. F., Gourley, B. C., and Olson, M. C. (1997). "A Cyclic Nonlinear Model for Concrete-Filled Tubes. I. Formulation. II. Verification," *J. of Struc. Eng.*, ASCE, Vol. 123, No. 6, June, pp. 736-754.

Hajjar, J. F. (2000). "Concrete-Filled Steel Tube Columns under Earthquake Loads," *Progress in Structural Engineering and Materials*, Vol. 2, No. 1, pp. 72-82.

Kradzig, W. B., Meyer, I. F., and Meskouris, K. (1989), "Damage Evolution in Reinforced Concrete Members Under Cyclic Loading," Proceedings Fifth International Conference on Structural Safety and Reliability (ICOSSAR 89), San Fransisco, California, August 7-11, 1989, Vol. II, pp. 795-802.

Mehanny, S. S. F. and Deierlein, G. G. (2000). "Modeling of Assessment of Seismic Performance of Composite Frames with Reinforced Concrete Columns and Steel Beams," Report No. 135, John A. Blume Earthquake Engineering Center, Stanford University, August.

Morino S., Uchikoshi M., and Yamaguchi I. (2001). "Concrete-Filled Steel Tube System-Its Advantages," *Steel Structures*, Vol. 1, pp. 33-44.

Tort, C. and Hajjar, J. F. (2003). "Damage Assessment of Concrete Filled Steel Tube Members and Frames for Performance-Based Design," Structural Engineering Report No. ST-03-1, Department of Civil Engineering, University of Minnesota, Minneapolis, Minnesota, April.

Varma, A. H., Ricles, J. M., Sause, R., Lu L. (2002). "Experimental Behavior of High Strength Square Concrete-Filled Steel Tube Beam-Columns," *J. of Struc. Eng.*, ASCE, Vol. 128, No. 3, March, pp. 309-318.

Yun, S., Hamburger, R. O., Cornell, C. A., and Foutch, D. A. (2002). "Seismic Performance Evaluation for Steel Moment Frames," *J. of Struc. Eng.*, ASCE, Vol. 128, No. 4, April, pp. 534-545.

Table 1: Damage Functions for Monotonically-Loaded Columns

Damage Level	Damage Function	Range of Parameters [L/D; D/t; f'_c; f_y; P_c/P_o]	Statistics [N; R^2; η; σ]
Steel Yielding	*for* $L/D \le 4$ $\frac{d_{cy}}{d_o} = 0.61\frac{P_s}{P_o} + 0.044$	*for* $L/D \le 4$ [2.0-4.2; 15.0-74.0; 19.8-119.0; 194.2-835.0; 0.16-0.86]	*for* $L/D \le 4$ [55; 0.51 ;0.38 ;0.16]
	for $L/D \ge 15$ $\frac{d_{cy}}{d_o} = 1.76\frac{P_s}{P_o} - 0.26$	*for* $L/D \ge 15$ [15.0-23.0; 20.3-36.6; 31.1-92.4; 290.0-413.0; 0.25-0.65]	*for* $L/D \ge 15$ [5; 0.97; 0.76; 0.33]
	$\frac{E_{cy}}{E_{total}} = 0.20\frac{P_s}{P_o} + 0.021\frac{L}{D} - 0.17$	[3.0-23.0; 15.0-73.7; 19.8-103.0; 194.2-835.0; 0.16-0.65]	[52; 0.54; 0.050; 0.14]
Concrete Crushing	*for* $L/D \le 5$ $\frac{d_c}{d_o} = 1.03\frac{P_c}{P_o} + 0.20$	*for* $L/D \le 5$ [2.0-5.6; 15.0-74.0; 20.6-119.0; 194.2-835.0; 0.16-0.86]	*for* $L/D \le 5$ [68;0.51; 0.67;0.27]
	for $L/D \ge 15$ $\frac{d_c}{d_o} = 1$	*for* $L/D \ge 15$ [15.4, 22.2; 28.6, 36.6; 92.4; 412.6, 413.0; 0.60,0.65]	*for* $L/D \ge 15$ [2; 1.0; 1.0; 0]
	$\frac{E_c}{E_{total}} = 0.28\frac{P_c}{P_o} + 0.022\frac{L}{D} - 0.14$	[2.0-22.2; 15.0-74.0; 20.6-119.0; 194.2-835.0; 0.19-0.86]	[56; 0.73; 0.092; 0.098]
Local Buckling	$\frac{d_{lb}}{d_o} = 2.68 \times (\frac{D}{t}\sqrt{\frac{f_y}{E_s}})^{-1.02}$	[3.0-5.0; 17.0-74.0; 19.8-119.0; 194.2-835; 0.14-0.81], $(D/t) \times \sqrt{f_y / E_s}$: 0.70-3.83	[35, 0.55,1.96, 1.71]
	$\frac{E_{lb}}{E_{total}} = 0.14\frac{L}{D} - 0.10\frac{D}{t}\sqrt{\frac{f_y}{E_s}} + 0.041$	[3.0-5.0; 17.0-74.0; 19.8-119.0; 194.2-835.0; 0.14-0.81], $(D/t) \times \sqrt{f_y / E_s}$: 0.70-3.83	[35, 0.60,0.35, 0.21]

Table 2: Geometric and Material Properties of the Specimens Generated for the Parametric Study of Deformation-Based Damage Index of Monotonically Loaded Column Tests

Spec.	*L/D*	*D/t*	f_y (MPa)	f'_c (MPa)	P_c/P_o	$\frac{D}{t}\sqrt{\frac{f_y}{E_s}}$	d_{cy}/d_o	d_c/d_o	d_{lbf}/d_o	μ
1	3.0	22.5	194.2	20.6	0.34	0.70	0.45	0.55	3.86	7.19
2	5.0	22.5	194.2	20.6	0.34	0.70	0.45	0.55	3.86	14.37
3	3.0	22.5	194.2	74.0	0.65	0.70	0.26	0.87	3.86	1.84
4	5.0	22.5	194.2	74.0	0.65	0.70	0.26	0.87	3.86	1.84
5	3.0	50.0	194.2	30.7	0.65	1.56	0.26	0.87	1.70	1.36
6	5.0	50.0	194.2	30.7	0.65	1.56	0.26	0.87	1.70	8.54
7	3.0	40.0	194.2	40.0	0.65	1.24	0.25	0.88	2.14	1.84
8	5.0	40.0	194.2	40.0	0.65	1.24	0.25	0.88	2.14	1.84
9	3.0	17.0	825.0	55.0	0.19	1.09	0.54	0.40	2.45	9.00
10	5.0	17.0	825.0	55.0	0.19	1.09	0.54	0.40	2.45	16.18
11	3.0	17.0	825.0	103.0	0.31	1.09	0.47	0.51	2.45	7.70
12	5.0	17.0	825.0	103.0	0.31	1.09	0.47	0.51	2.45	14.88
13	3.0	50.0	825.0	20.6	0.23	3.21	0.52	0.43	0.82	4.31
14	5.0	50.0	825.0	20.6	0.23	3.21	0.52	0.43	0.82	11.49
15	3.0	50.0	825.0	103.0	0.59	3.21	0.29	0.81	0.82	2.09
16	5.0	50.0	825.0	103.0	0.59	3.21	0.29	0.81	0.82	9.27

Table 3: Correlation of Performance Level and Damage Index [after Mehanny and Deierlein (2000)]

Performance Level	Deformation-Based Damage Index	Energy-Based Damage Index
Immediate Occupancy	< 0.8	< 0.30
Life Safety	0.8-1.5	0.30-0.60
Near Collapse	1.5-5.0	0.60-0.95
Collapse Prevention	> 5.0	> 0.95

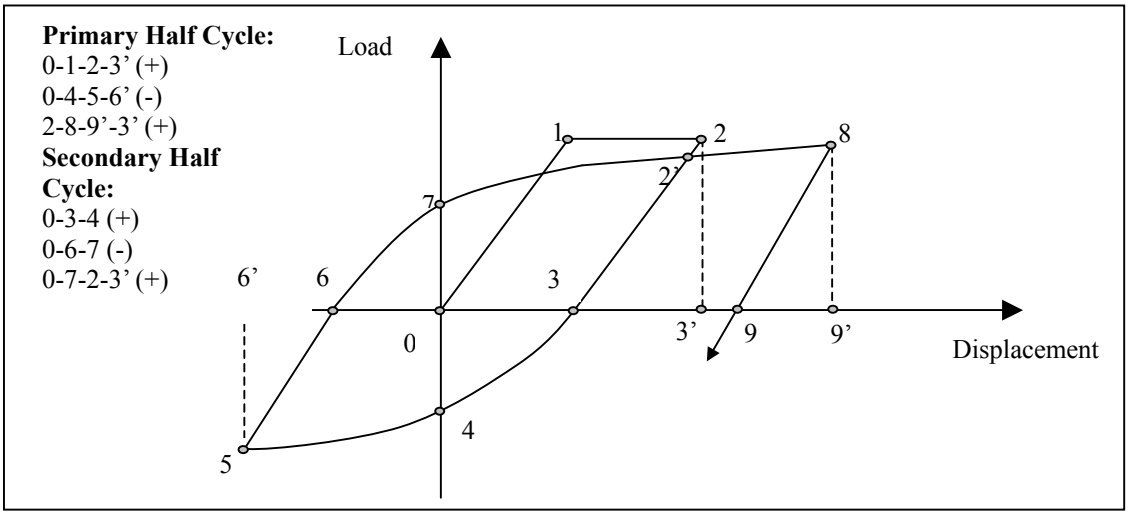

Figure 1: Definition of Primary and Secondary Cycles [after (Kradzig et al., 1989)]

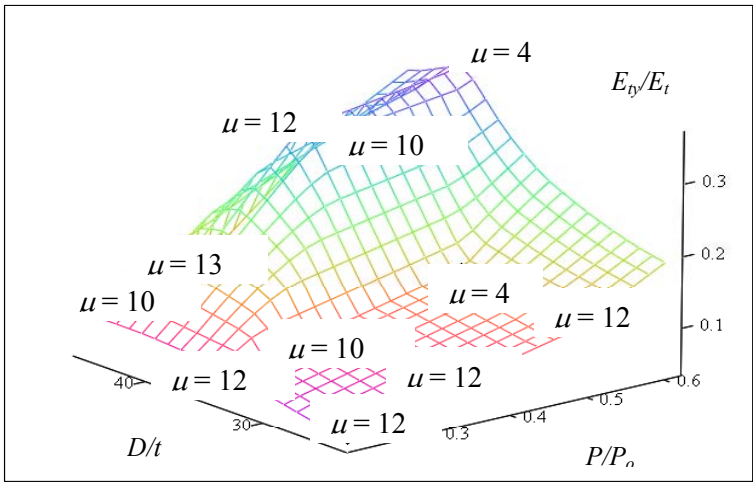

Figure 2: Comparison of D/t and P/P_o vs. E_{ty}/E_{total} for Monotonically-Loaded (MII) Beam-Column Tests

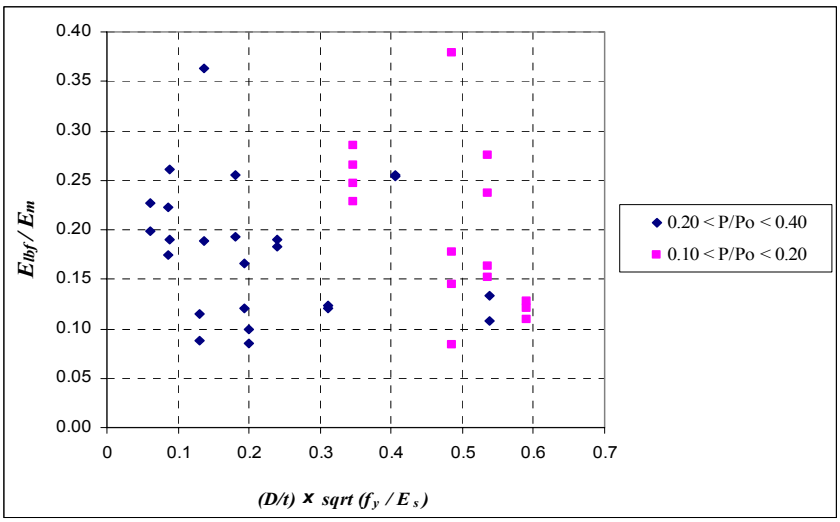

Figure 3: Comparison of $(D/t)\times(f_y/E_s)$ vs. E_{lbf}/E_m for Cyclically-Loaded Beam-Column Tests

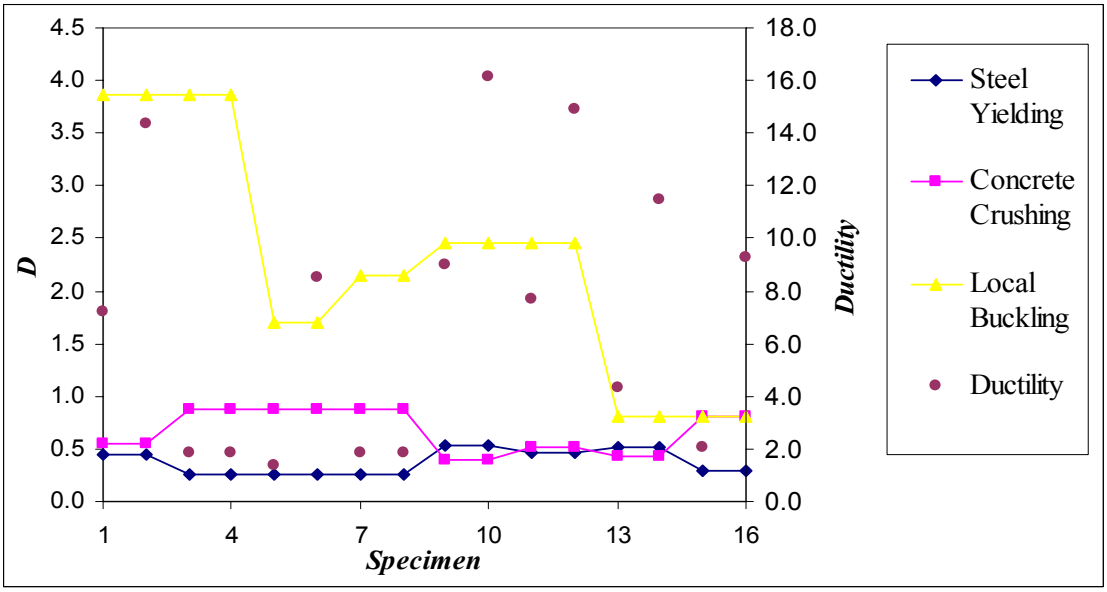

Figure 4: Comparison of Deformation-Based Damage Indices for Monotonically-Loaded Columns

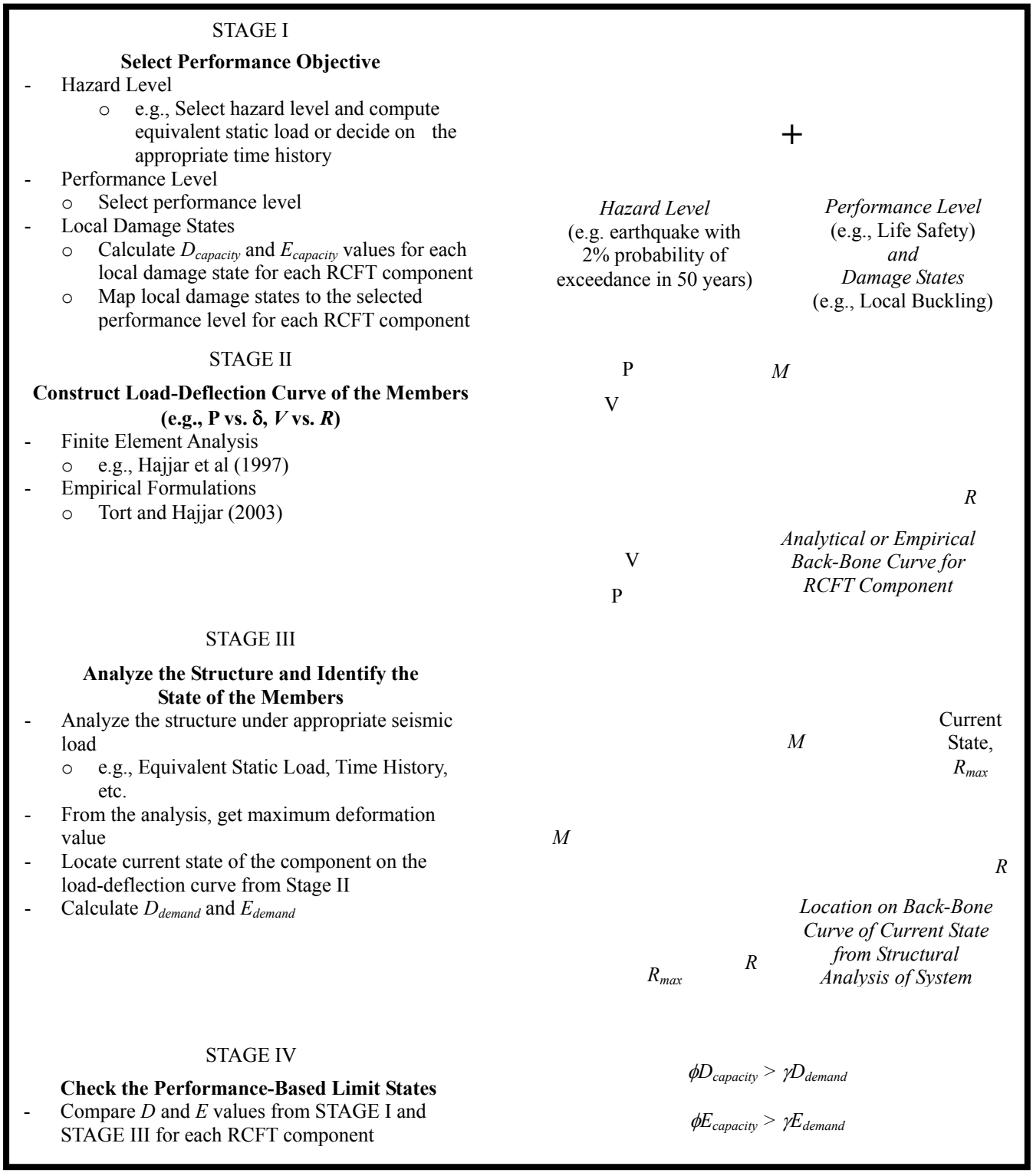

Figure 5: Intended Performance-Based Design Methodology